applied sciences

MDPI

Article

Cost-Effective Temperature Sensor for Monitoring the Setting Time of Concrete

Leticia Presa Madrigal [1,*], Juan Antonio Rodríguez Rama [1], Domingo A. Martín Sánchez [1,2], Jorge L. Costafreda Mustelier [1], Miguel Ángel Sanjuán [3] and José Luis Parra y Alfaro [1]

[1] Escuela Técnica Superior de Ingenieros de Minas y Energía, Universidad Politécnica de Madrid, 28003 Madrid, Spain; jrodriguez@alumnos.upm.es (J.A.R.R.); domingoalfonso.martin@upm.es (D.A.M.S.); jorgeluis.costafreda@upm.es (J.L.C.M.); joseluis.parra@upm.es (J.L.P.y.A.)
[2] Laboratorio Oficial para Ensayos de Materiales de Construcción (LOEMCO), C/Eric Kandell 1, 28906 Getafe, Spain
[3] Department of Science and Technology of Building Materials, Civil Engineering School, Technical University of Madrid, 28040 Madrid, Spain; masanjuan@ieca.es
* Correspondence: leticia.presa.madrigal@upm.es

Abstract: Concrete and Portland cement-based products are the most widely used materials in the construction industry. According to the Global Cement and Concrete Association (GCCA), 14 billion cubic meters of concrete are consumed worldwide every year. Knowledge of their properties is essential to ensure the quality of concrete products and structures. Knowing the evolution of certain parameters related to their durability makes it possible to prevent situations that affect compliance with quality requirements. Thanks to advances in IoT (Internet of Things) technologies, it is possible to know the evolution of these parameters in real time. The following work pursues the development and application of a prototype to monitor the setting time of concrete. This equipment provides real-time measurements, taking advantage of the Internet of Things (IoT) technology, allowing effective monitoring of the thermal behavior of concrete during its setting process. By measuring the temperature of the process and evaluating the resistance acquired during the setting time, we can correlate these two parameters, thus ensuring their correct evolution and allowing quick action to avoid future problems. For the development of this work, temperature measurements were made during the setting of 12 concrete specimens corresponding to four different mixtures (two types of cement with and without additives), assessed at three setting ages (28, 90, and 180 days). Through detailed experimental tests, the sensor was accurately and reliably validated, showing its ability to detect temperature changes, indicating the initial and final setting time. In addition, it was observed that the integration of the DS18B20 sensor does not compromise the structural properties of the concrete. The prototype's cost-effectiveness, efficiency, and easy installation make it a valuable tool for construction professionals, offering an innovative solution to ensure the quality and durability of the concrete. This breakthrough could represent a significant step towards the digitalization and improvement of construction processes, with direct implications for the efficiency and sustainability of modern infrastructures.

Keywords: digitalization; IoT; sensor; concrete; setting time measure

Citation: Presa Madrigal, L.; Rodríguez Rama, J.A.; Martín Sánchez, D.A.; Costafreda Mustelier, J.L.; Sanjuán, M.Á.; Parra y Alfaro, J.L. Cost-Effective Temperature Sensor for Monitoring the Setting Time of Concrete. *Appl. Sci.* **2024**, *14*, 4344. https://doi.org/10.3390/app14114344

Academic Editor: Vahid Afroughsabet

Received: 29 March 2024
Revised: 16 May 2024
Accepted: 17 May 2024
Published: 21 May 2024

1. Introduction

Portland cement and cement-based products are the main material used in civil engineering, due to its durability and mechanical properties, which positions it as one of the most widely used materials with a global production of 4.1 billion tons in 2022 [1]. Civil engineering structures built with concrete play an important role in the socioeconomic activity of a country, and it is essential to know precisely the properties of these materials and ensure compliance with quality standards to prevent these structures from reaching the end of their useful life prematurely due to problems caused by poor curing or problems

such as cracking, carbonation, corrosion, efflorescence, etc. [2–5], thus compromising the safety of users and the preservation of public and private assets, making the ability to monitor and maintain the integrity of civil structures imperative [6].

Numerous internationally standardized tests seek to establish minimum criteria to ensure the quality of these materials; However, such tests are often expensive and take a considerable amount of time. Furthermore, these tests provide real-time data at specific times, requiring additional inspections to assess the long-term condition of the material. In structural quality inspection programs, it is still predominant to perform a periodic visual inspection [7], limited to the observation of visible damage at discrete points [8], which is insufficient to maintain the health of civil infrastructures and the safety of users [9].

In contrast, the application of techniques to monitor the properties of cement and concrete allows real-time information to be obtained, providing greater certainty about the condition of the material.

A critical factor during concrete setting is temperature, which is closely related to its structural quality. The strength and durability of concrete change during the hydration process and are significantly influenced by temperature and moisture content at early ages [10–13]. The exothermic chemical reaction that accompanies cement hydration, known as hydration heat, raises the temperature of the concrete, influencing thermal stress and crack formation in early stages [14]. The curing temperature, a critical parameter in the progress of cement hydration, influences the stability, transformation of hydrates, and development of concrete strength [15]. A high temperature causes a further decrease in moisture content at an early age, thus affecting the concrete properties in the short and long term [16]. Variation affects the reaction rate and produces non-homogeneous precipitation of hydrates, increasing porosity and modifying the composition of the pore solution [17–20].

Temperature dependence is a significant challenge on construction sites where knowledge of the strength of concrete is required. Measuring the maturity of concrete is commonly considered to estimate its strength, as it is an excellent indicator of the development of strength in situ and is directly related to the hydration temperature. In this context, obtaining direct, in situ, and real-time measurements of concrete temperature is one of the main challenges in monitoring the structural state of civil infrastructures. In addition, it enables continuous monitoring during the curing process, allowing problems to be identified in time and appropriate corrective measures to be applied.

The monitoring of temperature within the construction sector is feasible thanks to IoT, or the Internet of Things, technologies, which have emerged as a solution to connect devices and objects of daily life to the network, facilitating communication between these, as well as the collection of data for analysis and future applications. Its uses are many, ranging from remote control of home appliances to real-time health monitoring. The advancement of IoT technologies has been enabled due to the miniaturization of sensors and wireless connectivity. The use of technologies such as Bluetooth and Wi-Fi have enabled efficient and secure communication between devices, which, in turn, improves efficiency and reduces operating costs.

There are several technologies that can be used which are being studied and even marketed for temperature monitoring in concrete structures, such as passive wireless sensors, negative temperature coefficient (NTC) thermistors, resistance temperature detectors (RTD), thermocouples, thermometers, and sensors based on semiconductors, among others [21,22]. However, many of these devices are only suitable for monitoring temperature on the surface or immediately around the concrete structure, excluding temperatures within a concrete matrix. Other trending options are fiber optics and Bragg Gratings in Fiber Optics (FBG) [23–28], which have advantages such as multiplexing capability, small dimensions, and easy installation. Although the cost of the FBG sensor is acceptable due to advanced manufacturing technology, an interrogator is required for its use, which is relatively expensive compared to other electrical data acquisition systems. In addition, the FBG interrogator is usually fragile and has strict requirements for operating temperatures and relative humidity, and another computer is needed for data storage [29].

Sensors are commonly placed on the reinforcement bars before concrete is poured; the device works by measuring temperature and humidity, focusing on the assessment of the temperature increase inside the concrete structure from the time of pouring to the completion of the project. The alkaline environment of concrete, the interference of the concrete material with the data transmission, the stability of the signal transmission, database size, scale issues, and limited lifetime are some of the main issues identified during the study of the use of sensors in concrete [30–33].

In this research, a system for concrete temperature measurements has been developed with low-cost commercial sensors, a microprocessor, and a platform for data collection and real-time visualization, in order to provide the industry with a continuous measurement system that ensures optimal curing conditions for concrete structures. With the implementation of this system, we aim to facilitate the use of this type of non-destructive tests that allow real-time monitoring of the curing state of our concrete and detect possible deficiencies during curing due to its low cost, easy installation, and intuitive operation.

2. Materials and Methods

Four mixtures were prepared with different percentages of cement substitution by zeolite (15% and 25%) and two reference cements (CEM I and CEM II). In addition, 20% of the coarse aggregate was replaced by recycled concrete aggregate in one of the samples to evaluate whether there were significant differences in the performance of the concrete. Nine specimens were prepared for each of the mixtures following the UNE-EN 12390-2 standard of 2020 [34]. The specimens were cured in water inside a humid chamber to ensure the control of environmental factors such as temperature (20 °C ± 2 °C) and humidity (≥95%). Of the nine specimens, three were used for each age of breakage (28 and 180 days) and one was monitored for each age. All specimens (with and without sensors) were subsequently subjected to the hardened concrete test to determine their compressive strength as described in the UNE-EN12390-3 standard of 2020 [35].

A total of twelve sensors (one sensor for each mixture and curing age) were used to measure the temperature every five minutes during the setting process. In addition, an environmental sensor was used to measure the water temperature.

The dosage used for the preparation of the 9 cylindrical specimens of 150 × 300 mm is shown in Table 1.

Table 1. Dosage for 9 cylindrical specimens.

Material	Quantity (kg)
Cement	17.2
Fine aggregate	55
Coarse aggregate	43.5
Water	9.7
Superplasticizer	0.14

From the above dosage, substitutions of different materials were made to obtain the different mixtures as shown in Table 2.

Table 3 shows the characterization of the composition of the materials used by X-ray diffraction.

Particle size analysis of the aggregates used was carried out, with the results shown in Figure 1.

Table 2. Dosage of mixtures.

	Sample 1 *	Sample 2 *	Sample 3 *	Sample 4 *
CEM II	100%	75%		
CEM I			85%	85%
Zeolite		25%	15%	15%
Fine aggregate	100%	100%	100%	100%
Coarse aggregate	100%	100%	100%	80%
Concrete aggregate recycled				20%
Water added (mL) [1]		600	300	800

* Every sample is made up of three specimens named as 1-2-3; [1] For samples with zeolite content, water was added to the original dosage until a consistency similar to that of the reference sample was achieved.

Table 3. Composition of materials by XRF.

Composition (%)	CEM I	CEM II	Standard Fine Aggregate	Fine Aggregate	Coarse Aggregate	Recycled Concrete Aggregate	Zeolite
Al_2O_3	4.76	5.09	1.55	0.73	1.23	4.25	9.64
BaO	0.08	0.09	0.02	0.02	0.01	0.04	<0.01
CaO	>60.00	>60	0.16	18.50	21.20	10.85	1.20
Cr_2O_3	0.01	0.01	<0.01	<0.01	<0.01	0.14	<0.01
Fe_2O_3	3.57	2.7	0.61	0.25	0.48	1.94	1.27
K_2O	1.04	0.96	0.61	0.36	0.31	1.46	2.14
MgO	1.47	1.8	0.09	0.16	0.55	0.45	1.09
MnO	0.05	0.07	0.01	0.01	0.01	0.02	<0.01
Na_2O	0.30	0.14	0.19	<0.01	0.02	0.54	3.63
P_2O_5	0.12	0.16	0.03	0.01	0.03	0.05	<0.01
SO_3	3.24	2.95	0.02	0.06	0.05	0.32	<0.01
SiO_2	19.86	19.84	95.44	64.34	59.17	72.25	68.42
SrO	0.03	0.11	<0.01	0.01	0.01	0.02	<0.01
TiO_2	0.25	0.24	0.06	0.04	0.14	0.16	0.11
LOI	3.77	6.45	0.47	14.84	17.49	7.91	11.58

For temperature monitoring, the DS18B20 sensor (Zhiwei Robotics Corp. from Shanghai, China), was used, due to its versatility, simple programming, low cost, and resistance to humid environments. It is a digital Celsius thermometer that provides 9 to 12 bits, with 64-bit memory (equivalent to 8 bytes) to store the unique identifier or address of every sensor and a non-volatile top alarm function programmable by the user. It is compatible with Arduino and has three pins: Vcc, GND, and DQ, which in this case corresponds to the data pin. The sensor can be encapsulated, i.e., sealed in a watertight wrapper, and there is also waterproof probe. The DS18B20 sensors support 3 to 5.5 V power and 9-bit, 10-bit, 11-bit, and 12-bit resolutions (12-bit resolution is the default). The range of temperature values it can measure are from -55 °C to 125 °C, with an accuracy of ± 0.5 °C from -10 °C to +85 °C; outside this range, the variation could be greater.

The sensor was made of stainless steel, and was 6 mm in diameter and 30 mm in length. The behavior of the sensor was previously analyzed by the Testing and Calibration Laboratory (LECEM) of the ETSIME-UPM, where the ENAC calibration certificate was obtained.

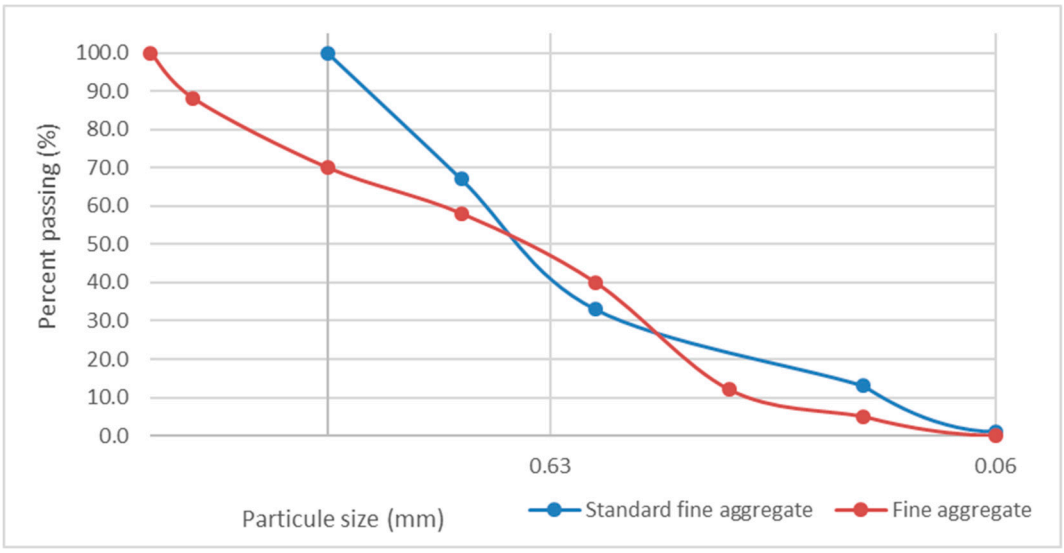

(**a**)

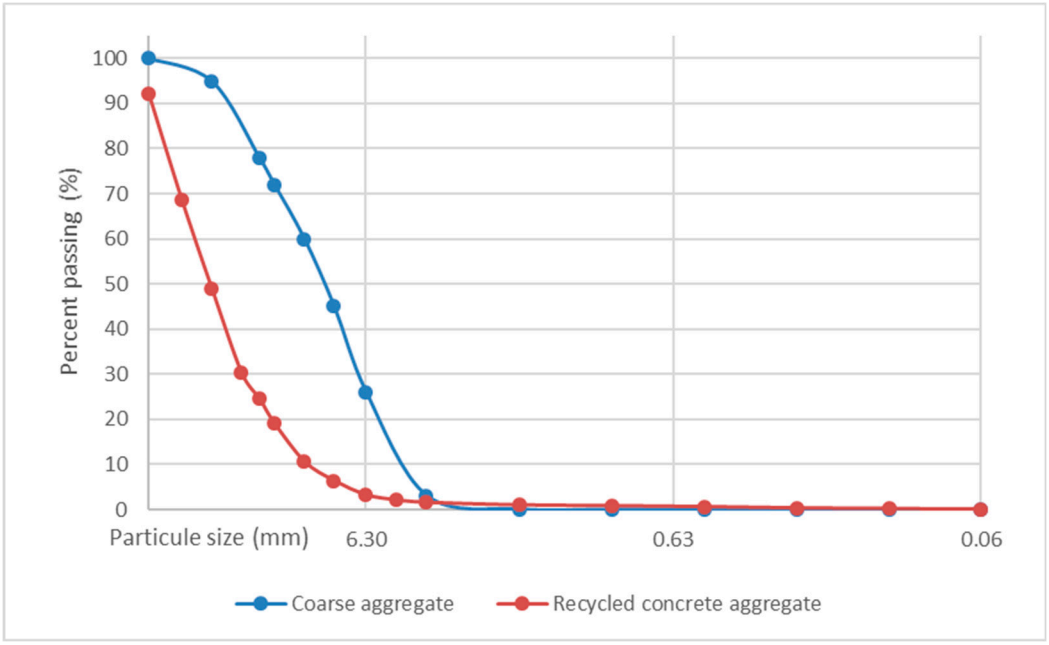

(**b**)

Figure 1. Particle size distribution. (**a**) comparison of the particle size distribution of the standard fine aggregate and the fine aggregate used. (**b**) comparison of particle size distribution of natural coarse aggregate and recycled concrete aggregate.

In addition, a BME280 (Adafruit, from New York, NY, USA) environmental sensor was used to verify that the conditions were suitable for curing the samples.

The communication protocol makes it possible to control several sensors distributed over a wide area with a single microprocessor. Data transmission was carried out via Wi-Fi connection.

The data was transmitted by Wi-Fi connection to our IoT platform, known as Tellus IoT (V 2.1), which allows storage to take place in the cloud as well as real-time visualization of the data generated by the project (Figure 2). This IoT infrastructure enables the effective management of real-time data to optimize processes, making it the digital core for informed and up-to-date decision-making [36].

Figure 2. Conceptual diagram of communication system and IoT platform operation.

Two separate tests were carried out in order to be able to adjust the parameters as necessary. In the first trial, two Node MCU Lolin v3 microcontrollers and a power supply were set up. The environmental microcontroller was physically connected via a cable to the BME280 sensor inside the wet chamber. The other microcontroller was connected to the different DS18B20 sensors via the electrical terminals. The seven sensors inside the wet chamber measured the temperature of the specimen mixture during the setting time and the temperature of the water. The connection diagram and the final schematic of the first prototype are shown in Figures 3 and 4.

In the second test, a power supply was established for a Lolin v3 Node MCU microcontroller. To this end, the previous design was optimized by making small necessary modifications, as shown in Figure 5.

The integration of the sensors, together with the intercommunication and real-time data analysis capability provided by the Tellus UPM Ecosystem, allow us to obtain a solution that can adapt and respond to the specific needs of the industry, leading the way towards sustainable and technologically advanced innovations.

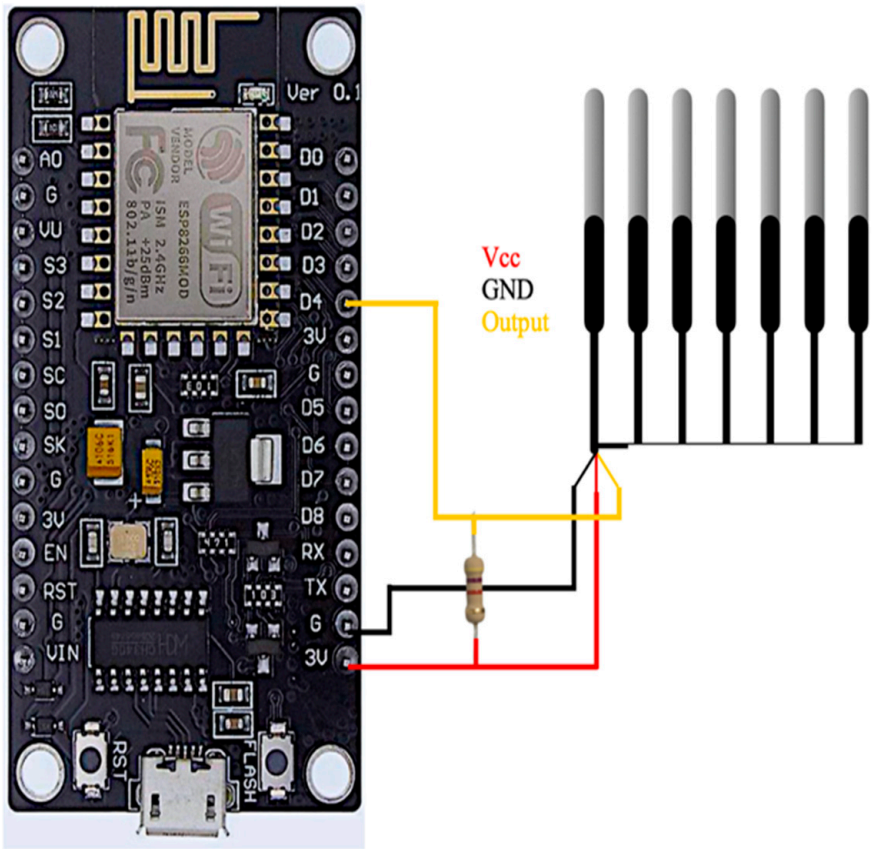

Figure 3. Schematic of DS18B20 sensor connection.

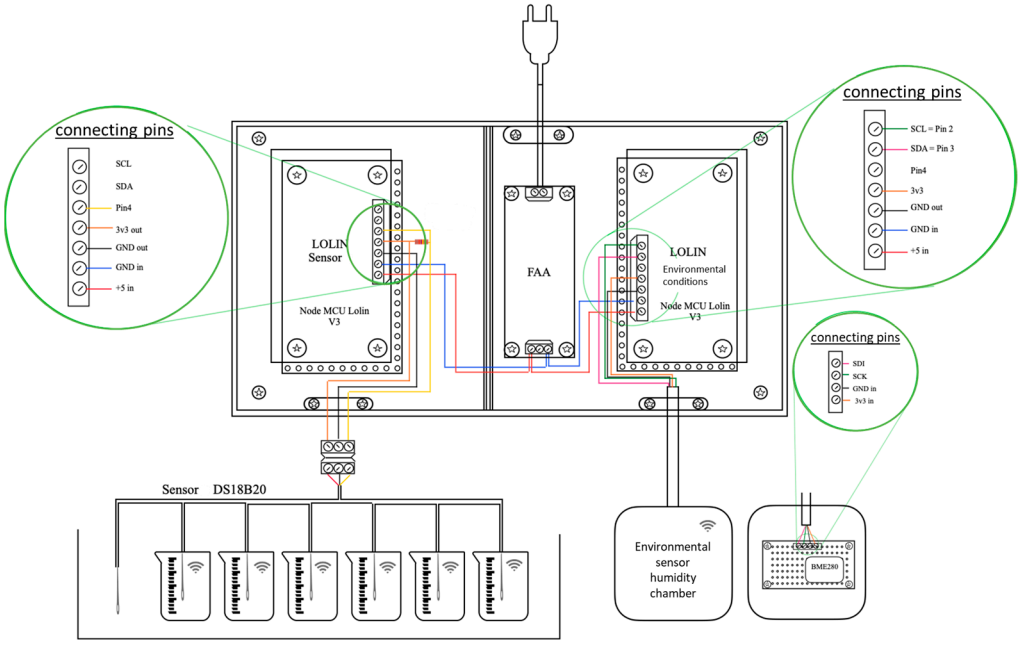

Figure 4. Final prototype design for test 1.

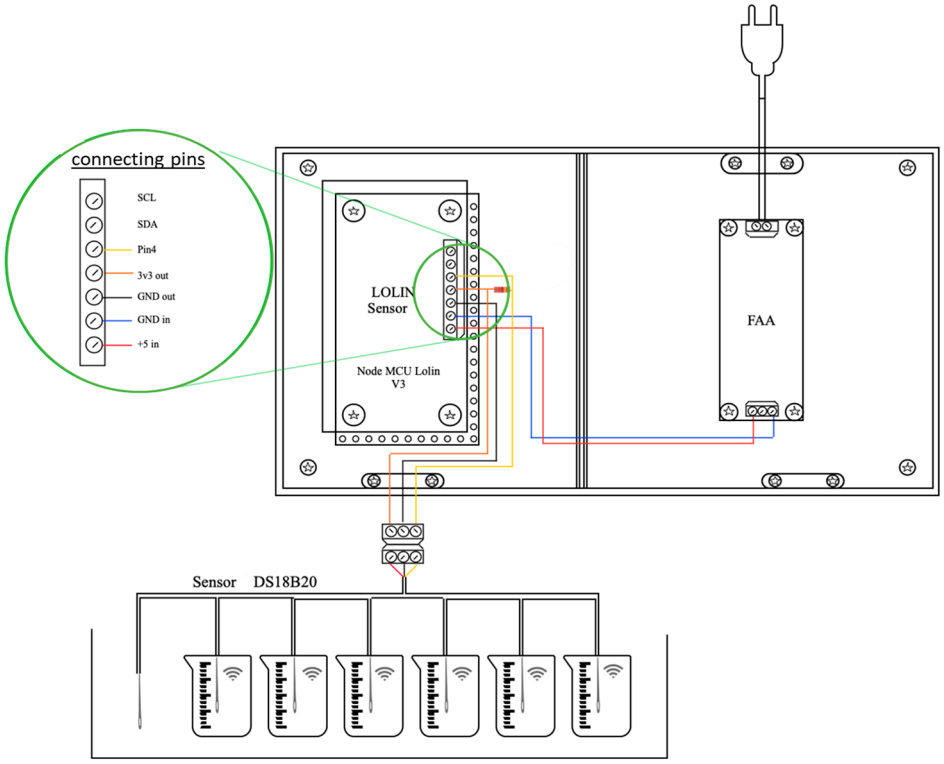

Figure 5. Final prototype design for test 2.

3. Results

During the first hours of setting, the most significant exothermic reactions occur and the greatest amount of heat is released, so its analysis provides us with a large amount of information. In order to be able to clearly visualize what happens during this period and how a different dosage of additions affects the process itself, the temperature probes of the specimens of the first test have been graphed in Figure 6.

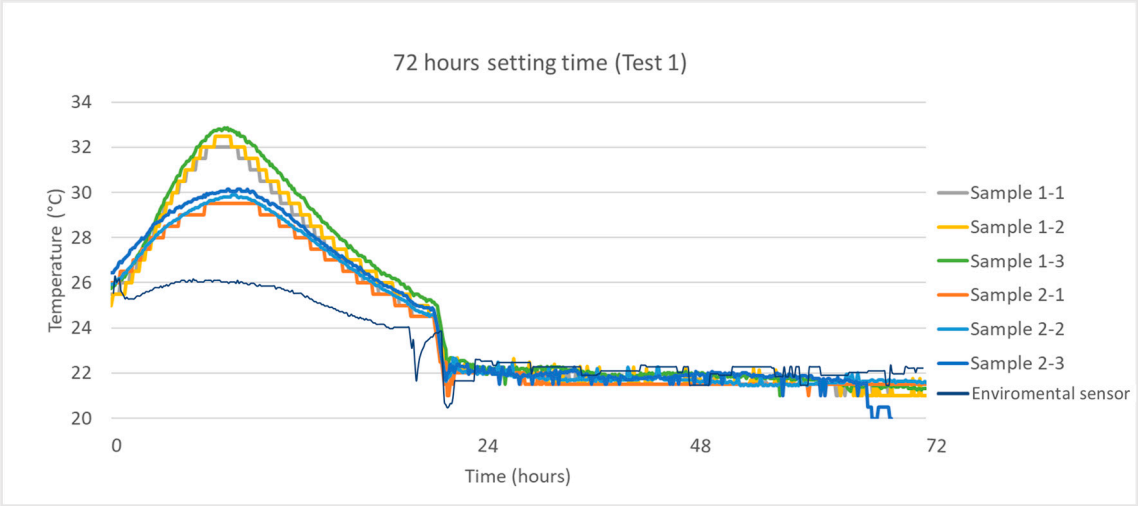

Figure 6. First 72 h of setting test 1.

Two distinct trends can be observed. In the probes corresponding to sample 1, a maximum temperature of 32.88 °C was reached during setting, higher than that measured in the probes corresponding to sample 2, which reached a maximum temperature of 30.13 °C. In conclusion, zeolite-containing mixtures reach lower temperatures.

During the second test, it can be seen in Figure 7 that the probes in sample 4 reached a peak temperature of 24.4 °C, higher than the probes belonging to sample 3, which reached a maximum temperature of 21.88 °C. This temperature difference can be attributed to the presence of recycled concrete aggregate, as its components can react in cement hydration processes generating greater hydration heat. In probe number 5 (corresponding to water), it can be seen that, unlike the sensors that measure inside the specimens, there was no increase in temperature due to the exothermic reactions of the cement hydration.

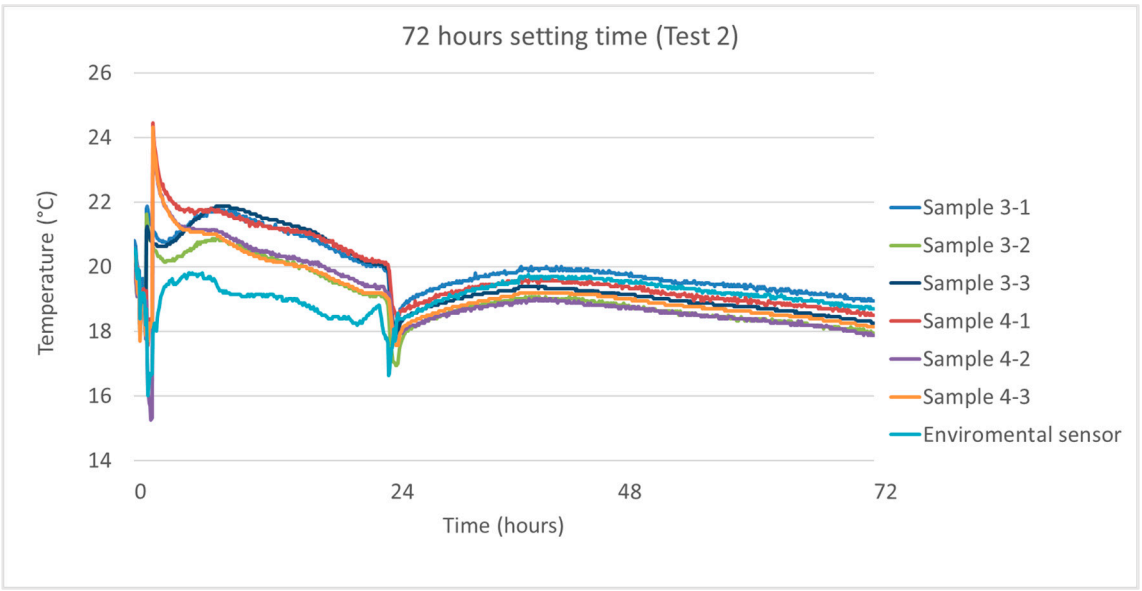

Figure 7. First 72 h of setting test 2.

In both cases, a sudden drop in temperature was observed over 24 h, which coincides with the introduction of the specimens into the water bath inside the wet chamber, since the curing water was at a stable temperature of 20 ± 2 °C.

One of the times of interest is the 28-day cure, which was expected to correspond to advanced strength gain. Figures 8 and 9 show the temperature values obtained in the two tests.

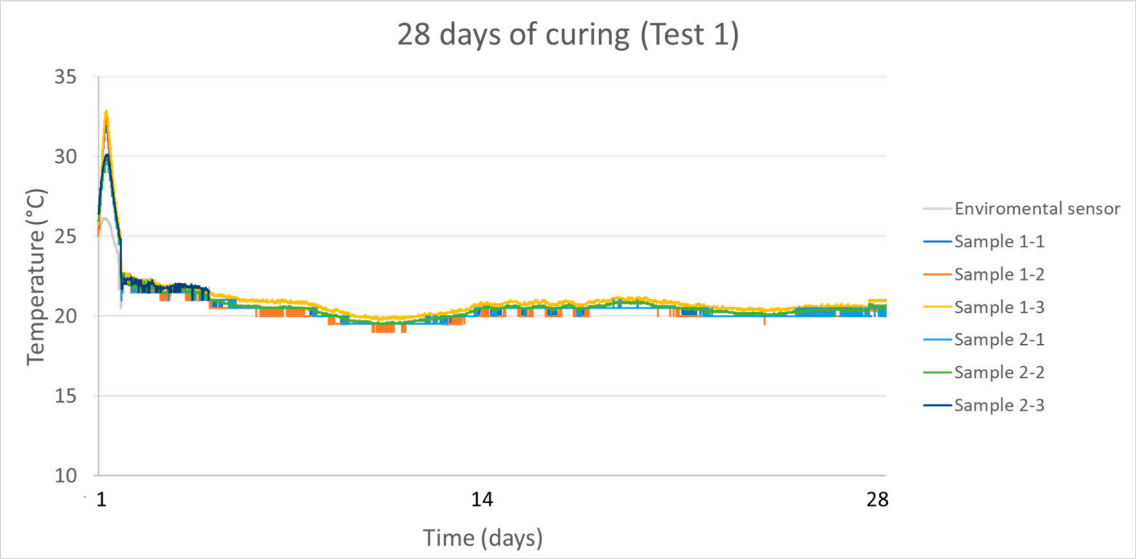

Figure 8. First 28 days of setting test 1.

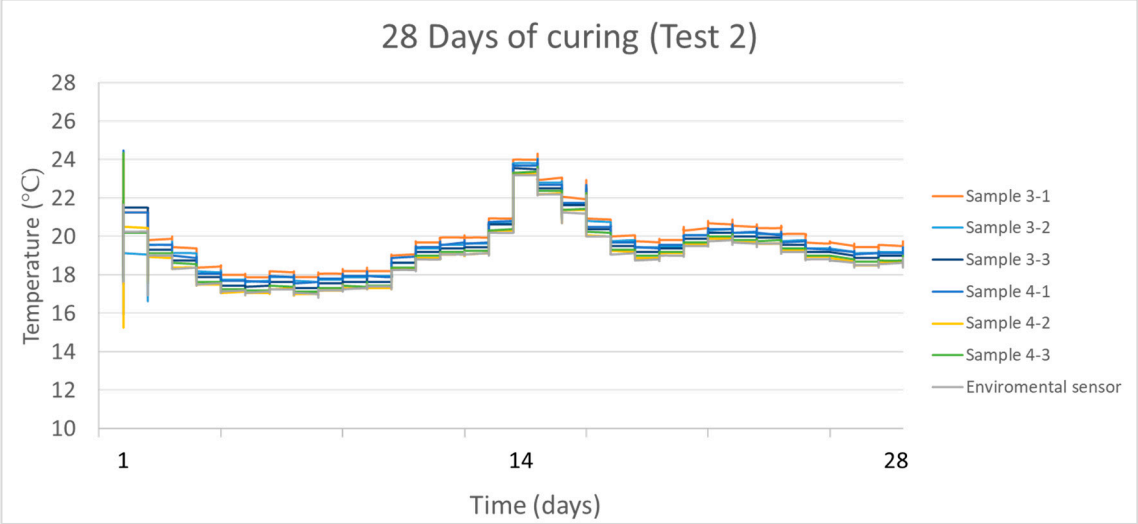

Figure 9. First 28 days of setting test 2.

It can be observed that, unlike the first hours of setting, the temperature sensors of the different samples showed identical behavior to that of the ambient temperature sensor during curing up to 28 days.

Figures 10–13 show the results obtained during 180 days of temperature monitoring.

These graphs are a quick visual way to represent the results. In each representation, the same type of mixture is reflected, so all three sensors should measure the same; even then, we see that there is a small difference in the measured values. Following the recommendations of the LECEM-ETSIME UPM studies, an adjustment was applied to the readings of the DS18B20 sensors with a correction of +0.4 °C and an uncertainty of ±0.050 °C (where K = 2, i.e., the uncertainty has been multiplied by two to obtain a 95% confidence interval), and it was assumed that the uncertainty is the same for all measurements. The average temperature difference ranged from 0.1 °C to 0.4 °C, which coincides with the uncertainty

mentioned above. Therefore, the three sensors measured the same temperature and the difference in values between them was due to the intrinsic temperature of the instrument.

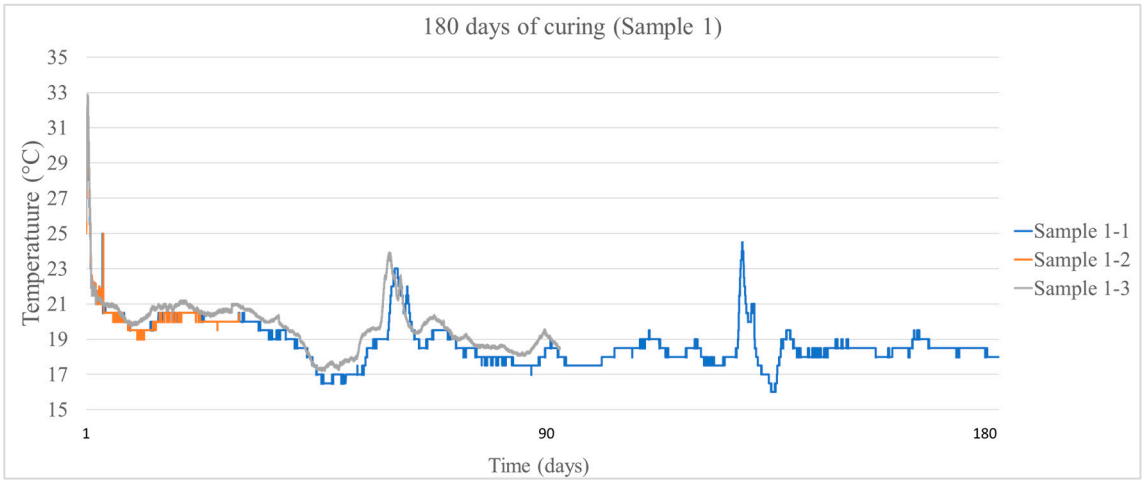

Figure 10. Comparison of temperature values obtained during monitoring of sample 1.

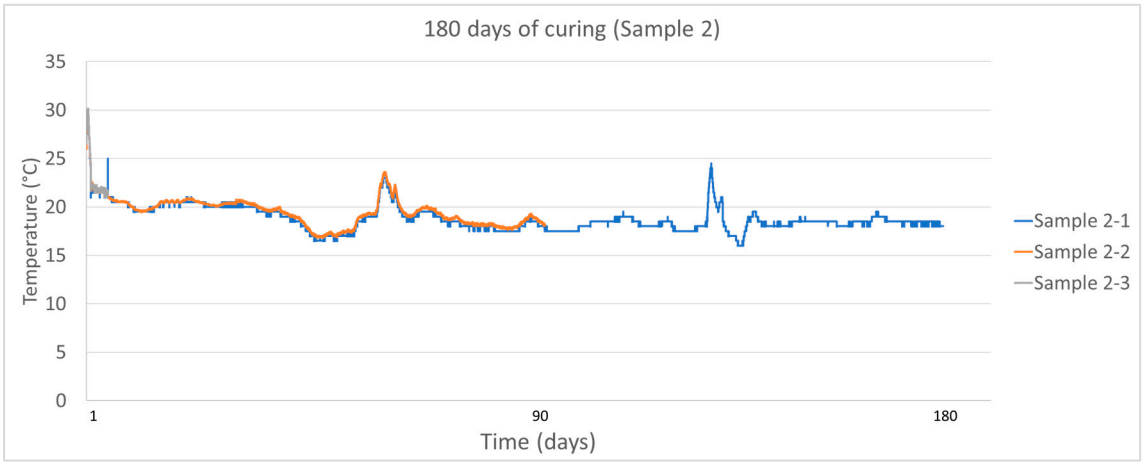

Figure 11. Comparison of temperature values obtained during monitoring of sample 2.

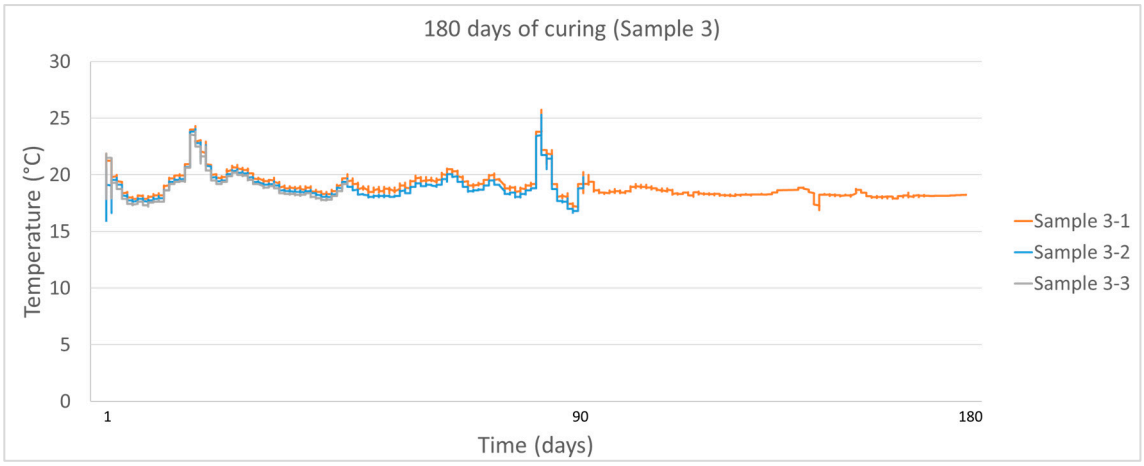

Figure 12. Comparison of temperature values obtained during monitoring of sample 3.

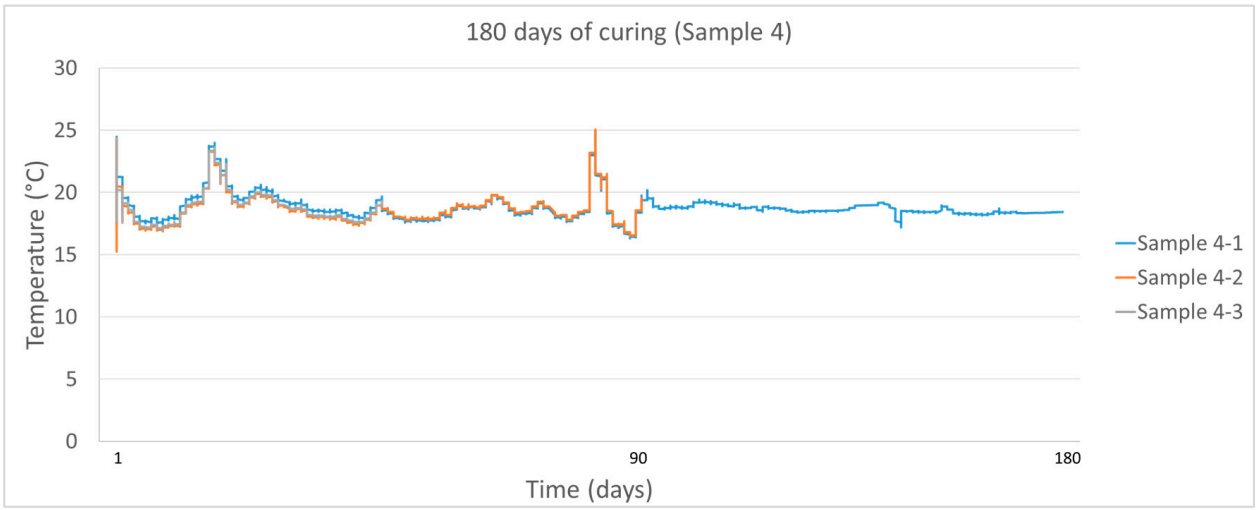

Figure 13. Comparison of temperature values obtained during monitoring of sample 4.

To analyze the results, a comparison was made between the various samples during the 180 days of monitoring, which can be seen in Figure 14.

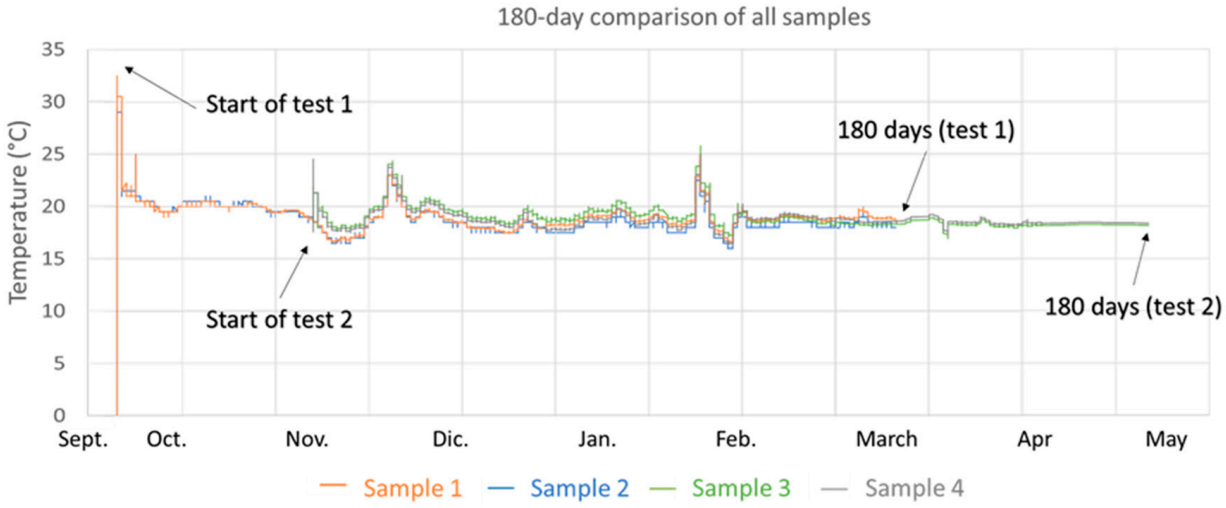

Figure 14. Comparison of 180-day monitoring results of the four samples.

As already mentioned, the assembly of the specimens of tests 1 and 2 was carried out in different periods of time, so to make the comparison, the results have been superimposed, coinciding the period in which the specimens coexisted.

At 28 and 180 days of curing, the compressive strength test was performed on the mortar specimens.

In Figure 15, a large variation can be observed between the compressive strengths of the different materials, with the reference samples (sample 1 and CEMII) being the ones with the highest strength.

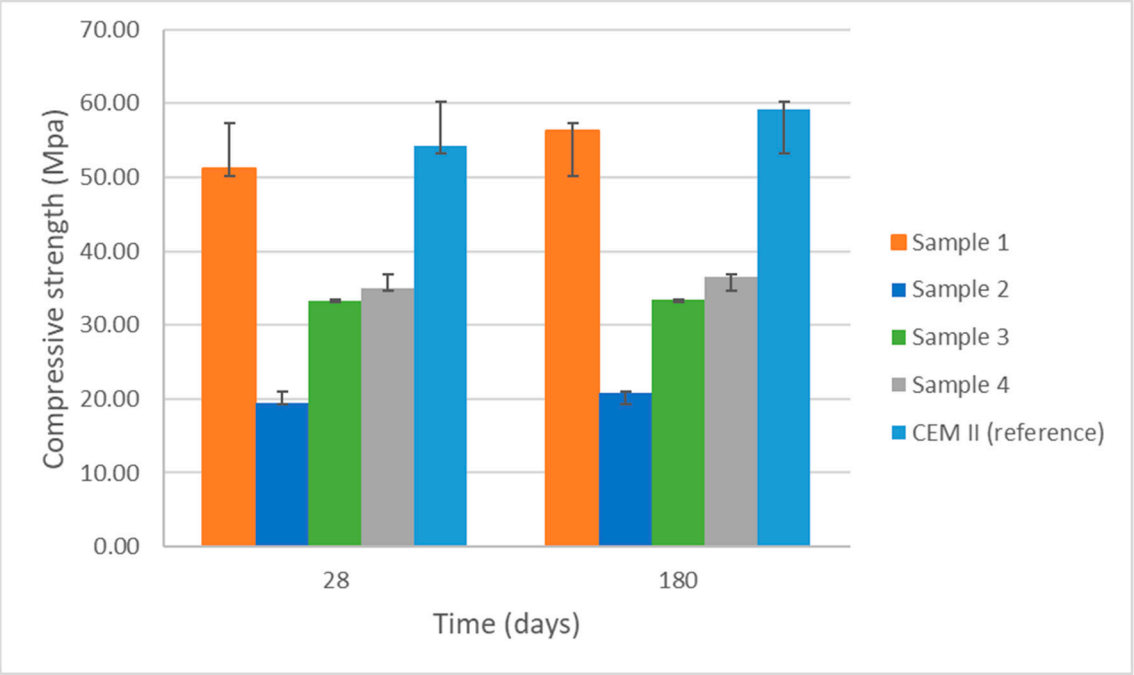

Figure 15. Compressive strength results at 28 and 180 days.

4. Discussion

Within the scope of this study, one of the primary objectives is to validate the capability of the employed sensors to withstand the curing conditions of concrete over an extended duration, ensuring successful monitoring of concrete specimens. During the temperature monitoring of the concrete specimens, it has been observed that the sensors used have correctly recorded the temperature up to the breaking age of 180 days. This shows that the sensors used are sufficiently resistant to water and concrete components for proper operation.

Furthermore, the aim is to verify the proper measurement of curing temperature, analyze the obtained results, and compare them across the various materials under investigation.

Type II cement samples without zeolite additions have obtained higher maximum temperature values during hydration than the rest of the samples. A high temperature in the early stages of hydration is associated with higher early resistance values, while concretes with lower hydration temperatures reach higher strengths at older ages [20]. This fact is consistent with research on cements with additions of pozzolanic materials, in which it is observed that maximum strengths are reached at later ages compared to reference cements [37,38]. If we compare the results obtained in the compressive strength test, we can see that the short-term strength of concrete specimens with additions is indeed lower than the strength of the reference cement. Pozzolanic materials give concrete remarkable performance in hot climates where the negative effect of temperature is partly reduced by the pozzolanic reaction, its weak heat of hydration, and its high activation energies [39]. As the temperature conditions in which the specimens were made were low, the contribution of zeolites may not be as significant as in hot climates, since pozzolanic materials help to improve the performance of mortars and the resistance of concrete when exposed to higher-than-normal temperatures, particularly in the range of 35–50 °C [40]. Therefore, climatic conditions should be considered a relevant parameter when selecting the most suitable materials to plan their use.

It is important to note that the temperatures obtained by the specimens do not exceed 50 °C in any of the cases, a value at which hydration problems begin to occur due to the formation of heterogeneously distributed hydrates, leading to the formation of larger pores [17], a denser C-S-H, and a more equidistant morphology of the ettringite [41].

In the comparison of the results obtained in the monitoring of the four specimens at 180 days, it can be observed that, except for the initial periods, the values coincide in both tests for the coexistence period. This provides us with two conclusions; on the one hand, that it is indeed in the initial curing periods that most exothermic hydration reactions occur, and on the other hand, that the variations at later ages correspond to external factors (curing water temperature and ambient temperature) and not to intrinsic processes of cement curing.

If we compare the compressive strength test results and the temperatures obtained, it can be observed that the concrete sample without zeolite additions is the one that obtains the highest value of early compressive strength and, in addition, it is the one that demonstrates the greatest increase in long-term strength. This sample corresponds to the one with the highest temperature in the first hours of curing. This temperature can be related to a greater number of hydration reactions and therefore greater resistance. Sample 2, which is the second sample with the highest hydration temperature, is the one with the lowest resistance, so it could be said that in the case of samples containing zeolite, no correlation has been found between the temperature in the first hours of curing and the resistances obtained. But, as explained, there are many factors, including the ambient temperature, that can alter the hydration temperatures that a concrete can reach. If we compare samples 3 and 4, which were made on the same day, it can be observed that the sample with the highest resistance (sample 4) is also the one that reached the highest temperature in the first hours of hydration. Therefore, it could be established that there is a correlation between the hydration temperature and the expected resistance.

All the previous remarks are consistent with the expected results within the type of material used, indicating that the temperature measurements obtained can be considered correct. Based on the results obtained, it can be inferred that the sensors are correctly measuring the temperature; therefore, the sensors used together with the system for measuring, storing, and displaying the results prove to be suitable for use within the industry, providing a low cost and sufficiently accurate measurement alternative.

5. Conclusions

In this study, the setting temperature of concrete specimens with different compositions has been monitored using low-cost sensors and a digital platform that allows the visualization of the results in real time. During the monitoring of the temperature of the concrete samples, it has been observed that the sensors, used accurately, recorded the temperature until the samples reached an age of 180 days, at which point their compression break occurred. This result indicates that the sensors are sufficiently resistant to water and concrete components to maintain proper operation.

From the comparison of the temperature results obtained during the monitoring of the specimens at 180 days, two conclusions can be drawn. First, most exothermic hydration reactions occur during the first curing periods, and second, the variations observed in more advanced stages are related to external factors rather than intrinsic cement curing processes, since there are no significant variations between the temperatures of the different specimens at later ages.

After comparing the results obtained in the compressive strength tests, climatic conditions have been revealed as important parameters to be taken into account when selecting the appropriate materials for application, since these conditions can influence the behavior of the concrete.

After observing the compressive strength results and correlating them with the maximum temperature reached during the setting process, it can be observed that it is very likely that there is a correlation between the hydration temperature and the expected resistance under similar processing conditions, despite not being able to compare specimens.

Author Contributions: Conceptualization, L.P.M., J.A.R.R., J.L.C.M. and D.A.M.S.; methodology, L.P.M., J.A.R.R., J.L.C.M. and D.A.M.S.; software, J.A.R.R., J.L.C.M. and D.A.M.S.; validation, J.L.C.M., J.L.P.y.A., M.Á.S. and D.A.M.S.; formal analysis, L.P.M., J.A.R.R., J.L.C.M., J.L.P.y.A., M.Á.S. and

D.A.M.S.; investigation, L.P.M., J.A.R.R., J.L.C.M., J.L.P.y.A., M.Á.S. and D.A.M.S.; resources, J.L.C.M., J.L.P.y.A., M.Á.S. and D.A.M.S.; data curation, L.P.M. and J.A.R.R.; writing—original draft preparation, L.P.M., J.A.R.R., J.L.C.M. and D.A.M.S.; writing—review and editing, L.P.M., J.A.R.R., J.L.C.M., J.L.P.y.A., M.Á.S. and D.A.M.S.; supervision, J.L.C.M., J.L.P.y.A., M.Á.S. and D.A.M.S.; project administration, J.L.C.M., J.L.P.y.A., M.Á.S. and D.A.M.S.; funding acquisition, J.L.C.M., M.Á.S. and D.A.M.S. All authors have read and agreed to the published version of the manuscript.

Funding: This research received no external funding.

Institutional Review Board Statement: Not applicable.

Informed Consent Statement: Not applicable.

Data Availability Statement: Data available on request due to restrictions. The data presented in this study are available on request from the corresponding author. The data are not publicly available due to privacy reasons.

Acknowledgments: We extend our sincere gratitude to LECEM for their support in the calibration of the instrumentation, as well as to LOEMCO for generously providing us with access to their facilities for our tests. Their expertise and support have contributed significantly to the success of our research.

Conflicts of Interest: The authors declare no conflicts of interest.

References

1. U.S. Geological Survey. *Mineral Commodity Summaries 2023*; U.S. Geological Survey: Reston, VA, USA, 2023; 210p. [CrossRef]
2. Gjørv, O.E. Durability of concrete structures. *Arab. J. Sci. Eng.* **2011**, *36*, 151–172. [CrossRef]
3. Page, C.L.; Page, M.M. (Eds.) *Durability of Concrete and Cement Composites*; Elsevier: Amsterdam, The Netherlands, 2007.
4. Hooton, R.D.; Bickley, J.A. Design for durability: The key to improving concrete sustainability. *Constr. Build. Mater.* **2014**, *67*, 422–430. [CrossRef]
5. Sakiyama FI, H.; Lehmann, F.; Garrecht, H. Structural health monitoring of concrete structures using fibre-optic-based sensors: A review. *Mag. Concr. Res.* **2021**, *73*, 174–194. [CrossRef]
6. Farrar, C.R.; Worden, K. An introduction to structural healthmonitoring. *Philos. Trans. R. Soc.* **2007**, *365*, 303–315. [CrossRef]
7. Li, J.; Mechitov, K.A.; Kim, R.E.; Spencer, B.F. Efficient timesynchronization for structural health monitoring using wirelesssmart sensor networks. *Struct. Control Health Monit.* **2016**, *23*, 470–486. [CrossRef]
8. Phares, B.M.; Washer, G.A.; Rolander, D.D.; Graybeal, B.A.; Moore, M. Routine highway bridge inspection condition documentation accuracy and reliability. *J. Bridge Eng.* **2004**, *9*, 403–413. [CrossRef]
9. Cho, S.; Giles, R.K.; Spencer, B.F., Jr. System identification of a historic swing truss bridge using a wireless sensor network employing orientation correction. *Struct. Control Health Monit.* **2015**, *22*, 255–272. [CrossRef]
10. Hemming, P.; Esa, N. *Measurement of Relative Humidity and Temperature in a New Concrete Bridge vs. Laboratory Samples*; Research Report; Technical Research Center of Finland, VTT Building Technology Concrete Materials: Espoo, Finland, 1999.
11. Paulson, J.; Farhang, A. Measurements on the moisture state in a heavily trafficked concrete flat slab repaired with bonded concrete overlay. In Proceedings of the Nordic Mini-Seminar of the Nordic Concrete Federation, Espoo, Finland, 22 August 1997.
12. Pihlajavaara, S.E.; Paroll, H. Effect of carbonation on the measurement of humidity in concrete. In Proceedings of the 2nd international CIB/RILEM Symposium on Moisture Problem in Buildings, Rotterdam, The Netherlands, 10–12 September 1974; Volume 12.
13. Kim, J.K.; Lee, S.C. Moisture diffusion of concrete considering selfdesiccation at early ages. *J. Cem. Concr. Res.* **1999**, *29*, 1921–1927. [CrossRef]
14. Portland Cement Association. *Portland Cement, Concrete, and Heat of Hydration, Concrete Technology Today*; Portland Cement Association: Washington, DC, USA, 1997; Volume 18.
15. Rojas, M.F.; Cabrera, J. The effect of temperature on the hydration rate and stability of the hydration phases of Metakaolin–Lime–Water systems. *Cem. Concr. Res.* **2002**, *32*, 133–138. [CrossRef]
16. Terril, J.M.; Richardson, A.R. Nonlinear moisture profiles and shrinkage in concrete members. *Mag. Concr. Res.* **1986**, *38*, 220–225. [CrossRef]
17. Kjellsen, K.O.; Detwiler, R.J.; Gjørv, O.E. Development of microstructures in plain cement pastes hydrated at different temperatures. *Cem. Concr. Res.* **1991**, *21*, 179–189. [CrossRef]
18. Kjellsen, K.O.; Detwiler, R.J. Reaction kinetics of Portland cement mortars hydrated at different temperatures. *Cem. Concr. Res.* **1992**, *22*, 112–120. [CrossRef]
19. Escalante-Garcia, J.I. Nonevaporable water from neat OPC and replacement materials in composite cements hydrated at different temperatures. *Cem. Concr. Res.* **2003**, *33*, 1883–1888. [CrossRef]
20. Lothenbach, B.; Matschei, T.; Möschner, G.; Glasser, F.P. Thermodynamic modelling of the effect of temperature on the hydration and porosity of Portland cement. *Cem. Concr. Res.* **2008**, *38*, 1–18. [CrossRef]

21. Mathas, C. Temperature Sensors-The Basics. 2011. Available online: https://www.digikey.com.au/en/articles/techzone/2011/oct/temperature-sensors-thebasics (accessed on 16 January 2024).
22. Huynh, T. Fundamentals of thermal sensors. In *Thermal Sensors*; Jha, C.M., Ed.; Springer: Berlin/Heidelberg, Germany, 2015; pp. 5–42.
23. JLópez-Higuera, M.; Cobo, L.R.; Incera, A.Q.; Cobo, A. Fiber Optic Sensors in Structural Health Monitoring. *J. Light. Technol.* **2011**, *29*, 587–608. [CrossRef]
24. Merzbacher, C.; Kersey, A.; Friebele, E. Fiber optic sensors in concrete structures: A review. In *Optical Fiber Sensor Technology. Optoelectronics*; Grattan, K.T.V., Meggitt, B.T., Eds.; Imaging and Sensing Series; Springer: New York, NY, USA, 1999; pp. 1–24.
25. Glisic, B.; Inaudi, D. *Fibre Optic Methods for Structural Health Monitoring*; John Wiley & Sons: Hoboken, NJ, USA, 2008.
26. Luo, D.; Ismail, Z.; Ibrahim, Z. Added advantages in using a fiber Bragg grating sensor in the determination of early age setting time for cement pastes. *Measurement* **2013**, *46*, 4313–4320. [CrossRef]
27. Moyo, P.; Brownjohn, J.M.W.; Suresh, R.; Tjin, S.C. Development of fiber Bragg grating sensors for monitoring civil infrastructure. *Eng. Struct.* **2005**, *27*, 1828–1834. [CrossRef]
28. Jo, H.J.; Park, D.Y.; Kim, K.W.; Ahn, T.J. Real-time monitoring of concrete curing using fiber Bragg grating sensors: Strain and temperature measurement. *Sens. Actuators A Phys.* **2023**, *362*, 114650. [CrossRef]
29. Qiao, H.; Lin, Z.; Sun, X.; Li, W.; Zhao, Y.; Guo, C. Fiber optic-based durability monitoring in smart concrete: A state-of-art review. *Sensors* **2023**, *23*, 7810. [CrossRef]
30. Chung, D.D.L. A critical review of electrical-resistance-based self-sensing in conductive cement-based materials. *Carbon* **2023**, *203*, 311–325. [CrossRef]
31. Roshan, M.J.; Abedi, M.; Correia, A.G.; Fangueiro, R. Application of self-sensing cement-stabilized sand for damage detection. *Constr. Build. Mater.* **2023**, *403*, 133080. [CrossRef]
32. Halvorsen, G.T.; Farahmandnia, A. *The Willow Island Collapse: A Maturity Case Study, Temperature Effects on Concrete*; ASTM International: West Conshohocken, PA, USA, 1985.
33. Chang, C.Y.; Hung, S.S. Implementing RFIC and sensor technology to measure temperature and humidity inside concrete structures. *Constr. Build. Mater.* **2012**, *26*, 628–637. [CrossRef]
34. *UNE-EN 12390-2:2020*; Ensayos de Hormigón Endurecido. Parte 2: Fabricación y Curado de Probetas Para Ensayos de Resistencia. UNE: Madrid, Spain, 2020.
35. *UNE-EN 12390-3:2020*; Ensayos de Hormigón Endurecido. Parte 3: Determinación de la Resistencia a Compresión de Probetas. UNE: Madrid, Spain, 2020.
36. Rama, J.A.R.; Lázaro, A.M.; Martín Sánchez, D.A.; Lorenzo, J.M.; Barrio-Parra, F.; Fernández Gutiérrez del Álamo, L.J. 3D Printing as an Enabler of Innovation in Universities. Tellus UPM Ecosystem Case. In *Smart Cities. ICSC-Cities 2023. Communications in Computer and Information Science*; Nesmachnow, S., Hernández Callejo, L., Eds.; Springer: Cham, Switzerland, 2024; Volume 1938. [CrossRef]
37. Nagrockiene, D.; Girskas, G. Research into the properties of concrete modified with natural zeolite addition. *Constr. Build. Mater.* **2016**, *113*, 964–969. [CrossRef]
38. Zolghadri, A.; Ahmadi, B.; Taherkhani, H. Influence of natural zeolite on fresh properties, compressive strength, flexural strength, abrasion resistance, Cantabro-loss and microstructure of self-consolidating concrete. *Constr. Build. Mater.* **2022**, *334*, 127440. [CrossRef]
39. Ezziane, K.; Bougara, A.; Kadri, A.; Khelafi, H.; Kadri, E. Compressive strength of mortar containing natural pozzolan under various curing temperature. *Cem. Concr. Compos.* **2007**, *29*, 587–593. [CrossRef]
40. Mirza, W.H.; Noury, S.I.; Bedawi, W.H. Temperature on strength of mortars and concrete containing blended cements. *Cem. Concr. Compos.* **1991**, *13*, 197–202. [CrossRef]
41. Lothenbach, B.; Winnefeld, F.; Alder, C.; Wieland, E.; Lunk, P. Effect of temperature on the pore solution, microstructure and hydration products of Portland cement pastes. *Cem. Concr. Res.* **2007**, *37*, 483–491. [CrossRef]